

Double-spirals offer the development of pre-programmable modular metastructures

Mohsen Jafarpour^{1, *}, Stanislav N. Gorb¹, Hamed Rajabi^{2, 3}

¹ Functional Morphology and Biomechanics, Institute of Zoology, Kiel University,
Kiel, Germany

²Division of Mechanical Engineering and Design, School of Engineering, London South Bank University

³Mechanical Intelligence Research Group, South Bank Applied BioEngineering Research (SABER), School of Engineering, London South Bank University, London, UK

* Corresponding author: MJ, 0000-0002-6814-6802; m.jafarpour1992@gmail.com; mjafarpour@zoologie.uni-kiel.de

SG, 0000-0001-9712-7953; sgorb@zoologie.uni-kiel.de

HR, 0000-0002-1792-3325; rajabih@lsbu.ac.uk

16 **Abstract**

17 Metamaterials with adjustable, sometimes unusual properties offer advantages over conventional
18 materials with predefined mechanical properties in many technological applications. A group of
19 metamaterials, called modular metamaterials or metastructures, are developed through the
20 arrangement of multiple, mostly similar building blocks. These modular structures can be
21 assembled using prefabricated modules and reconfigured to promote efficiency and functionality.
22 Here, we developed a novel modular metastructure by taking advantage of the high compliance of
23 pre-programmable double-spirals. First, we simulated the mechanical behavior of a four-module
24 metastructure under tension, compression, rotation, and sliding using the finite-element method.
25 Then, we used 3D printing and mechanical testing to illustrate the tunable anisotropic and
26 asymmetric behavior of spiral-based metastructures in practice. Our results show the simple
27 reconfiguration of the presented metastructure toward the desired functions. The mechanical
28 behavior of single double-spirals and the characteristics that can be achieved through their
29 combinations make our modular metastructure suitable for various applications in robotics,
30 aerospace, and medical engineering.

31

32 **Keywords:** Mechanical intelligence, structured materials, functional design, finite-element
33 method, 3D printing.

34

1. Introduction

Structured materials with unprecedented tunable properties have been increasingly developed in recent years and found applications in robotics [1,2], electronics [3], energy harvesting systems [x1, x2], biomedical engineering [4], aerospace engineering [5,6], structural engineering [7], etc [8,9, x3]. These materials, which are referred to as metamaterials, are engineered to exhibit properties that are derived from their architecture, rather than constituent materials [10,11]. Negative swelling ratio [8], negative thermal-expansion coefficient [12], negative Poisson's ratio [13], negative moduli [14], anisotropic behavior [15,16], reversible non-linear deformability [17,18], programmability [19,20], and shape memorability [x4] are some of the obtained mechanical properties.

Modular metamaterials consist of rationally designed modules or unit cells linked to each other. In these materials, desired mechanical properties can be achieved by engineered deformation of the consisting modules [21-23]. Hence, knowing the characteristics of each module is crucial when developing a metamaterial. The geometry, material composition, and spatial arrangement of modules are key factors that determine the behavior of modular metamaterials under different boundary conditions and loadings. Structures used as modules for the development of modular metamaterials vary from rotating rigid shapes [24-27], the wide range of honeycomb designs [28-30], and re-entrant structures [31-33] to horseshoe-shaped structures [8], bio-inspired double-layer hinges [34], foldable obelisk-like units [21], helical structures [x5], and many other different designs [2,16,19,35,36].

The aim of this study is to investigate the potential of pre-programmable compliant double-spiral structures, which have been recently introduced by our team, when used as the modules of a metastructure. Adjustable design, multiple degrees of freedom, high extensibility, and reversible non-linear deformability are properties of the double-spirals that make them particularly interesting for the development of deformable structures [37]. We expect that pre-programmable double-spiral modules will enable us to control the mechanical properties of a metastructure in different directions in a passive-automatic way.

Using the finite-element method (FEM), we simulate the mechanical behavior of a four-module metastructure under different loading scenarios. We also manufacture two modular metastructures using 3D printing and illustrate their performance in practice. Our results show that the combination of different double-spirals can lead to the tunable anisotropy, asymmetric behavior, pre-programmable shape change, spatial heterogeneity, and simple reconfiguration of the developed metastructure.

68 2. Methods

69 2-1. Modeling and finite-element analysis

70 Following the method adopted by Jafarpour et al. [37], we used the equation of logarithmic spirals
71 in the polar coordinate system (equation 1) to plot spiral curves using the programming software
72 MATLAB (MathWorks).

$$73 \quad r = r_0 e^{-k\theta}, \quad (1)$$

74 In the above equation, r_0 is the radius of the spiral at $\theta=0$, and k is the polar slope [38].

75 We plotted two logarithmic spirals with different initial radii ($r_{0,1}=13.5$ mm and $r_{0,2}=15.0$ mm
76) but an equal polar slope ($k=0.2$) from 0 to 1.5 pi radians. We then rotated them around the
77 origin of the coordinate system by pi radian to generate two other spirals. These four spiral curves
78 formed two spiral surfaces (**Fig. 1a**). After connecting the bases and the ends of spirals with straight
79 lines, the plot was imported to the finite-element software package ABAQUS/Standard v. 6.14
80 (SIMULIA) to develop the two-dimensional (2D) numerical model of the first double-spiral, named
81 double-spiral 1 (**Fig. 1b**).

82 The same procedure was used to develop a geometrically different double-spiral to investigate
83 the behavior of a combination of double-spirals employed as the modules of a modular
84 metastructure. We set the initial thickness, polar slope, and angle of rotation of the double-spiral 2
85 to be 3 mm ($r_{0,2}-r_{0,1}=15-12=3.0$ mm), 0.1, and 3 pi radians, respectively (**Fig. 1b**). The values
86 of the design variables were selected to obtain models with significantly different geometries.
87 Double-spiral 1 is extremely shorter, thinner, and more curved compared to double-spiral 2.

88 A modular metastructure, in which double-spiral modules were connected to blocks forming a
89 square, was designed here (**Fig. 1c**). We employed two models of each double-spirals 1 and 2 to
90 develop a four-module metastructure (**Fig. 1d**). We used this planar model to simulate its
91 mechanical behavior subjected to in-plane loading scenarios in Abaqus. The model was meshed
92 using four-node bilinear plane-stress quadrilateral elements with reduced integration (CPS4R). A
93 mesh sensitivity analysis was conducted to set the size of the elements. The 0.1-mm elements
94 resulted in accurate solutions in reasonable computational time. We used the self-contact
95 formulation in Abaqus to define the physical contacts between interacting surfaces [39].

96 The material properties of the thermoplastic polyurethane (Flexfill TPU 98A, Fillamentum
97 addi©tive polymers, Czech Republic) presented in **Table 1** were assigned to the model [40].

We used the Abaqus implicit solver to simulate the quasi-static behavior of the model under different loading scenarios. In all loading scenarios, the boundary conditions and loads were applied to the rigid blocks that were connected to the double-spirals. We avoided the large strain behavior of the elements and focused on reversible elastic deformations by limiting the load values. The following loading scenarios were simulated to characterize the performance of the spiral-based modular metastructure (**Fig. 2**):

(1) Tension: In this loading scenario, we once extended the model in the vertical and then in horizontal directions (with respect to the horizon). In both cases, we clamped the model on one side and pulled them on the opposite side until the double-spirals reached their maximum lengths (**Fig. 2a**).

(2) Compression: Here we compressed the model twice in two perpendicular directions, while the blocks on the opposite side were fixed (**Fig. 2b**). The compression was accomplished by applying a 2-N force.

(3) Rotation: Under rotation, the model was clamped at the two opposite blocks b1 and b3, and then only one of the two other blocks, i.e., b2, was subjected to a counterclockwise (CCW) moment (equal to 50 N.mm). Under the same loading and boundary condition, we then rotated the same block clockwise (CW) (**Fig. 2c**).

(4) Sliding: In this loading scenario, first we fixed the blocks on one side, here b1 and b4, and pulled one of the two other blocks, i.e., b3, downward by 50 mm, whereas b2 could move only vertically. We then clamped the model at a different side, i.e., b3 and b4, and pulled b2 horizontally to reach the same displacement, while b1 was restricted in the vertical direction (**Fig. 2d**).

2-2. Prototyping and mechanical testing

We manufactured two double-spirals from the numerical simulations, with an FDM 3D printer (Prusa i3 MK3S, Prusa Research, Praha, Czech Republic) to test their behavior and validate the results of the simulations. Double-spirals and fixtures were printed using a semi-flexible polyurethane filament (Flexfill TPU 98A, Fillamentum addi(c)tive polymers, Czech Republic) and a polylactic acid (PLA) filament (Prusa Research, Praha, Czech Republic), respectively. A ZwickiLine uniaxial testing machine (Zwick Roell, Ulm, Germany) equipped with a 500 N load cell (Xforce P load cell, Zwick Roell) was used to quantify the tensile behavior of the manufactured double-spirals. Three specimens of each double-spiral were tested each three times under the same loading and boundary conditions used in the numerical simulations of the tension (**Fig. 3**).

In the next step, we fabricated three double-spirals with distinct geometries using TPU filament and connected them to each other using connecting blocks made of PLA to develop modular metastructures with adjustable properties. We then tested their mechanical performance in practice. The values selected for design variables to obtain 3D models of the double-spirals, and 3D printing settings are given in **Table 2**. We assembled the printed parts to make a beam-like and a cubic metastructure and characterized their behavior in two different experiments. First, we fixed one end of the beam structure and applied a 250-N.mm moment to its other end to investigate its behavior in bending (**Fig. 4**). Then we used our uniaxial testing machine to quantify the compressive behavior of the cubic structure in three different directions (**Fig. 5**).

3. Results

3-1. Finite-element analysis

The double-spirals, their arrangement in the presented metastructures, and used loading scenarios are only a few examples of the many potential combinations of design, loading, and boundary conditions. We presented these specific combinations to illustrate the potentials of our modular metastructure for a range of practical applications.

The force-displacement diagram resulted from the simulation of tension showed that both tensile force and displacement in the vertical direction were about twice those in the horizontal direction (**Fig. 2a**). The force-displacement diagram corresponding to the compression showed that the metastructure was about six times more compliant under compression in the horizontal direction than in the vertical direction (**Fig. 2b**). These two loadings show the anisotropy of the developed metastructure.

Rotating a block of the model (b2 in **Fig. 2c**) in two opposite directions (CW and CCW) demonstrated its asymmetric behavior. Although the rotational deflections of b2 subjected to the same moment in two directions were not much different, the work required for the CCW deformation was about four times that for the CW deformation. The moment-rotation diagram shows the different stiffnesses of the metastructure in the two directions and their variations as the deformation increases (**Fig. 2c**).

The force-displacement diagrams illustrate the non-linear behavior of the metastructure, related to the specific phases of the deformation of the double-spirals under different loading scenarios (i.e., initial clearance, unrolling, and unfolding) [37]. The tension and rotation of the metastructure

in two different directions occur with an inversion of anisotropy. In tension, 0.5-N force is enough to unroll the double-spiral 1 horizontally and reach the high-stiffness unfolding phase (around 60-mm displacement). However, the vertical 0.5-N force extends the double-spiral 2 by only 10 mm. Nevertheless, the metastructure has higher extensibility in vertical direction when is subjected to larger tensile forces. The same scenario lies behind the inversion of anisotropy in the CW and CCW rotations of the metastructure.

We used the sliding scenario to indicate the behavior of the free block which was not loaded (b2 in the vertical sliding and b1 in the horizontal sliding, **Fig. 2d**). In the vertical loading, the displacement of the loaded block (b3) led to almost the same displacement of the free block (b2). However, in the horizontal loading, when we moved the block (b2) horizontally, the free block (b1) did not move and therefore the whole structure showed a different deformation pattern compared to the vertical loading (**Fig. 2d**).

3-2. Prototyping and mechanical testing

Here, we 3D printed the double-spirals used in numerical simulations and characterized their tensile behavior experimentally to verify the validity of the simulations. To this goal, we averaged the force-displacement curves from the experiments ($n=9$) and compared that to the numerical force-displacement curve (**Fig. 3**). We measured the quality of the fit by comparing the average force values resulted from the two methods at the same displacements. The comparisons show that for both double-spirals, a good agreement exists between the numerical and experimental J-shaped curves.

Two spiral-based metastructures were manufactured and tested in the next step. First, a beam-like modular metastructure was developed using double-spirals 1 and 2, that were horizontally connected to three blocks (**Fig. 4**). Two geometrically different double-spirals were employed in eight arrangements. Fixing one end of these structures and applying an equal moment to their free end resulted in different deformation patterns. The deflection of the middle point of beams varied from 21 mm to 55 mm, and the deflection of their tip varied from 53 mm to 118 mm. This demonstrates the asymmetric behavior and tunable structural stiffness of the developed structures that results from the different combinations of two double-spirals with different thicknesses, lengths, and polar slopes.

We then used the double-spirals 1, 2, and 3 to connect eight blocks in the form of a cube and developed three cubic modular metastructures (**Fig. 5a**). The first cube was made up of double-

spiral 1 only and was expected to have the same compressive stiffness in all three directions of the Cartesian coordinate system (**Fig. 5a-i**). The second cube, consisted of double-spirals 1 and 2, could behave the same in x and z directions, but different in y direction (**Fig. 5a-ii**).

To have a cubic metastructure with a specific mechanical characteristic in each direction, we used four of each double-spirals 1, 2, and 3 and developed the third cube (**Fig. 5a-iii**). The compressive behavior of this cube was quantified in three directions (**Fig. 5b**). We placed it between two plates and used a 100-N force to displace one plate towards the other one that was fixed. Repeating this test five times in each direction resulted in $2.9 (\pm 0.1)$ mm, $9.3 (\pm 0.3)$ mm, and $13.9 (\pm 0.4)$ mm displacement of the plate in x, y, and z direction, respectively. The compression of the double-spirals starts with a low-stiffness deformation phase, which originates from the free space between their coils, and continues with a gradual increase in the stiffness, which results from the contact between the coils [37]. The different compressive behaviors of the metastructure in x, y, and z directions are mainly caused by the different free space between the coils of the double-spirals and their thicknesses, which can be adjusted by changing the values of the design variables.

4. Discussion

Modular metastructures consisting of exchangeable modules can be used in different applications in which simple adjustability is a requirement. In this study, we used only two/three geometrically different double-spirals as modules of spiral-based modular metastructures to obtain distinct mechanical behaviors under the same load. Our results showed that the geometrical design variables of the double-spirals can be used to pre-program the behaviors observed. The spatial arrangement of the double-spirals, type of loading, and boundary condition determine the behavior of the spiral-based modular metastructure.

Using our double spirals in the developed metastructure enabled us to tune the stiffness of the metastructure in different directions, as well as how it changes during the application of the external loads. Our results illustrated the high reversible extensibility, variable stiffness, anisotropy, and asymmetric behavior of the developed metastructures. We could tune all these features by changing the design variables of the double-spirals and controlling the structural stiffness in each direction. These characteristics can be a great advantage to many engineering structures, such as mechanical hinges [41,42] biomedical implants [16], asymmetric casts and splints [43], flexible body armors [44], and load-bearing yet collision resistance kites [45].

Programmed shape change in response to mechanical loads is another interesting property of the metastructures. Shape changes can enable engineering structures to transform into predictable shapes when loaded, to change their performance and/or improve their efficiency [19,20]. In this study, the sliding loading scenario conducted horizontally and vertically resulted in two different deformation patterns (**Fig. 2d**). The difference is due to the internal boundary condition that double-spirals passively apply on each block. Numerical and experimental results suggest that this shape change can be pre-programmed by using different double-spirals with suitable geometrical design variables (**Fig. 2d, 3**). Varying the orientation of the modules from the horizontal and vertical directions to angled directions is another strategy that can also change the local boundary condition on the blocks and influence the behavior of the metastructure.

Since the modular metastructure developed here comprises individual modules, the dimensions of the metastructure can be easily changed by adding or removing double-spirals. Employing double-spirals with various mechanical behaviors in a larger structure could result in the spatial heterogeneity or gradient of properties. However, there is a constraint against increasing this heterogeneity. Complex aperiodic architectures could hinder the desired functionality of a structure and prevent its coherent and predictable response [19,x6]. Therefore, any design should provide a trade-off between the high level of controllability and complexity.

In this study, we presented the concept of using compliant double-spirals as the modules of a modular metastructure. The results showed the potential of double-spirals for this purpose. Considering that our simulations were conducted on small assemblies of double-spirals, future studies should focus on characterizing the behavior of spiral-based metastructures in large scales. A combinatorial design theory [19], an inverse-design method [x6], and a structural stiffness matrix-based computational method [x7,x8] are a few examples that can be used to predict the mechanical behavior of large spiral-based modular metastructures. Further investigations should examine the performance of the double-spirals with different geometries and material compositions under long-term loadings. Artificial intelligence (AI) has progressed the research on metamaterials and their applications [x3], and can be used in the future studies to obtain double-spirals with geometries optimized for specific applications. The arrangement of the modules in the developed metastructure is another factor that remains to be tested to improve the mechanical behavior of the metastructure.

5. Conclusion

In this article, we presented a modular metastructure that consists of compliant double-spirals and investigated its mechanical behavior under different loading scenarios. Our results showed that by combining double-spirals in specific configurations, we can exploit desired properties, including tunable anisotropy, asymmetric behavior, pre-programmable shape change, and spatial heterogeneity, besides the advantageous features of single double-spirals, such as simply adjustable design, multiple degrees of freedom, high extensibility, and reversible non-linear deformability. Furthermore, if any unexpected modification is necessary, the use of independently exchangeable modules in the modular metastructure makes its reconfiguration feasible. Individual double-spirals could be printed fast at low costs using a single material and be readily assembled. The metastructure presented in this study can offer an alternative design for engineered materials that are currently in use in various engineering fields. Compact, yet highly extensible double-spirals make the metastructure adequate for aerospace engineering products which need to be portable and stowable. Highly tunable non-linear deformations of the spiral-based metastructure in different directions suggest it could provide an efficient solution to the development of biomedical engineering devices for rehabilitation. The metastructure comprised pre-programmable double-spirals, which control the motion of components in a passive-automatic way, could be of particular interest in articulated robots.

Acknowledgements

The authors are grateful to Mr. Shahab Eshghi (Kiel University, Germany) for his helpful discussions.

Author contributions

MJ: Conceptualization; data curation; formal analysis; funding acquisition; investigation; methodology; validation; visualization; writing – original draft; writing – review & editing. **SG:** Conceptualization; funding acquisition; project administration; resources; supervision; writing – review & editing. **HR:** Conceptualization; methodology; project administration; supervision; writing – review & editing.

Conflicts of interest statement

The authors declare there are no conflicts of interest to disclose.

288

289 **Data accessibility**

290 The FE models can be made available on request; please contact MJ at:

291 m.jafarpour1992@gmail.com

292 mjafarpour@zoologie.uni-kiel.de

293

294 **Funding**

295 This study was financially supported by “Federal State Funding at Kiel University” to MJ. The
296 funders had no role in study design, data collection and analysis, decision to publish, or preparation
297 of the manuscript.

298

299 **References**

300 [1] Wang, L., Yang, Y., Chen, Y., Majidi, C., Iida, F., Askounis, E. and Pei, Q., 2018. Controllable
301 and reversible tuning of material rigidity for robot applications. *Materials Today*, 21(5), pp.563-
302 576. (doi: 10.1016/j.mattod.2017.10.010)

303 [2] Khajehtourian, R. and Kochmann, D.M., 2021. Soft adaptive mechanical metamaterials. *Frontiers*
304 *in Robotics and AI*, 8, p.121. (doi: 10.3389/frobt.2021.673478)

305 [3] Ma, Y., Feng, X., Rogers, J.A., Huang, Y. and Zhang, Y., 2017. Design and application of ‘J-
306 shaped’ stress–strain behavior in stretchable electronics: a review. *Lab on a Chip*, 17(10), pp.1689-
307 1704. (doi: 10.1039/C7LC00289K)

308 [4] Jang, K.I., Chung, H.U., Xu, S., Lee, C.H., Luan, H., Jeong, J., Cheng, H., Kim, G.T., Han, S.Y.,
309 Lee, J.W. and Kim, J., 2015. Soft network composite materials with deterministic and bio-
310 inspired designs. *Nature communications*, 6(1), pp.1-11. (doi: 10.1038/ncomms7566)

311 [5] Jefferson, G., Parthasarathy, T.A. and Kerans, R.J., 2009. Tailorable thermal expansion hybrid
312 structures. *International Journal of Solids and Structures*, 46(11-12), pp.2372-2387. (doi:
313 10.1016/j.jisolsolstr.2009.01.023)

314 [6] Morgan, J., Magleby, S.P. and Howell, L.L., 2016. An approach to designing origami-adapted
315 aerospace mechanisms. *Journal of Mechanical Design*, 138(5). (doi: 10.1115/1.4032973)

- 316 [7] Cveticanin L., 2020. Mechanical Metastructure in Structural Engineering: A Short Review.
317 *Current Trends in Civil & Structural Engineering*, 6(1). (doi: 10.33552/CTCSE.2020.06.000633)
- 318 [8] Zhang, H., Guo, X., Wu, J., Fang, D. and Zhang, Y., 2018. Soft mechanical metamaterials with
319 unusual swelling behavior and tunable stress-strain curves. *Science advances*, 4(6), p.eaar8535. (doi:
320 10.1126/sciadv.aar8535)
- 321 [9] Surjadi, J.U., Gao, L., Du, H., Li, X., Xiong, X., Fang, N.X. and Lu, Y., 2019. Mechanical
322 metamaterials and their engineering applications. *Advanced Engineering Materials*, 21(3), p.1800864.
323 (doi: 10.1002/adem.201800864)
- 324 [10] Yu, X., Zhou, J., Liang, H., Jiang, Z. and Wu, L., 2018. Mechanical metamaterials associated
325 with stiffness, rigidity and compressibility: A brief review. *Progress in Materials Science*, 94, pp.114-
326 173. (doi: 10.1016/j.pmatsci.2017.12.003)
- 327 [11] Bertoldi, K., Vitelli, V., Christensen, J. and Van Hecke, M., 2017. Flexible mechanical
328 metamaterials. *Nature Reviews Materials*, 2(11), pp.1-11. (doi: 10.1038/natrevmats.2017.66)
- 329 [12] Qu, J., Kadic, M., Naber, A. and Wegener, M., 2017. Micro-structured two-component 3D
330 metamaterials with negative thermal-expansion coefficient from positive constituents. *Scientific*
331 *reports*, 7(1), pp.1-8. (doi: 10.1038/srep40643)
- 332 [13] Kolken, H.M. and Zadpoor, A.A., 2017. Auxetic mechanical metamaterials. *RSC advances*, 7(9),
333 pp.5111-5129. (doi: 10.1039/C6RA27333E)
- 334 [14] Zadpoor, A.A., 2016. Mechanical meta-materials. *Materials Horizons*, 3(5), pp.371-381. (doi:
335 10.1039/C6MH00065G)
- 336 [15] Layman, C.N., Naify, C.J., Martin, T.P., Calvo, D.C. and Orris, G.J., 2013. Highly anisotropic
337 elements for acoustic pentamode applications. *Physical review letters*, 111(2), p.024302. (doi:
338 10.1103/PhysRevLett.111.024302)
- 339 [16] Xu, S., Shen, J., Zhou, S., Huang, X. and Xie, Y.M., 2016. Design of lattice structures with
340 controlled anisotropy. *Materials & Design*, 93, pp.443-447. (doi: 10.1016/j.matdes.2016.01.007)
- 341 [17] Mousanezhad, D., Ebrahimi, H., Haghpanah, B., Ghosh, R., Ajdari, A., Hamouda, A.M.S. and
342 Vaziri, A., 2015. Spiderweb honeycombs. *International Journal of Solids and Structures*, 66, pp.218-
343 227. (doi: 10.1016/j.ijsolstr.2015.03.036)
- 344 [18] Bonatti, C. and Mohr, D., 2017. Large deformation response of additively-manufactured FCC
345 metamaterials: From octet truss lattices towards continuous shell mesostructures. *International*
346 *Journal of Plasticity*, 92, pp.122-147. (doi: 10.1016/j.ijplas.2017.02.003)

- 347 [19] Coulais, C., Teomy, E., De Reus, K., Shokef, Y. and Van Hecke, M., 2016. Combinatorial
348 design of textured mechanical metamaterials. *Nature*, 535(7613), pp.529-532. (doi:
349 10.1038/nature18960)
- 350 [20] Konaković-Luković, M., Panetta, J., Crane, K. and Pauly, M., 2018. Rapid deployment of
351 curved surfaces via programmable auxetics. *ACM Transactions on Graphics (TOG)*, 37(4), pp.1-13.
352 (doi: 10.1145/3197517.3201373)
- 353 [21] Yang, N., Zhang, M., Zhu, R. and Niu, X.D., 2019. Modular metamaterials composed of
354 foldable obelisk-like units with reprogrammable mechanical behaviors based on multistability.
355 *Scientific reports*, 9(1), pp.1-7. (doi: 10.1038/s41598-019-55222-7)
- 356 [22] Liu, W., Jiang, H. and Chen, Y., 2022. 3D Programmable Metamaterials Based on
357 Reconfigurable Mechanism Modules. *Advanced Functional Materials*, 32(9), p.2109865. (doi:
358 10.1002/adfm.202109865)
- 359 [23] Mao, J.J., Wang, S., Tan, W. and Liu, M., 2022. Modular multistable metamaterials with
360 reprogrammable mechanical properties. *Engineering Structures*, 272, p.114976. (doi:
361 10.1016/j.engstruct.2022.114976)
- 362 [24] Grima, J.N., Alderson, A. and Evans, K.E., 2005. Auxetic behaviour from rotating rigid units.
363 *Physica status solidi (b)*, 242(3), pp.561-575. (doi: 10.1002/pssb.200460376)
- 364 [25] Attard, D. and Grima, J.N., 2008. Auxetic behaviour from rotating rhombi. *physica status solidi*
365 *(b)*, 245(11), pp.2395-2404. (doi: 10.1002/pssb.200880269)
- 366 [26] Gatt, R., Mizzi, L., Azzopardi, J.I., Azzopardi, K.M., Attard, D., Casha, A., Briffa, J. and Grima,
367 J.N., 2015. Hierarchical auxetic mechanical metamaterials. *Scientific reports*, 5(1), pp.1-6. (doi:
368 10.1038/srep08395)
- 369 [27] Jamalimehr, A., Mirzajanzadeh, M., Akbarzadeh, A. and Pasini, D., 2022. Rigidly flat-foldable
370 class of lockable origami-inspired metamaterials with topological stiff states. *Nature*
371 *communications*, 13(1), pp.1-14. (doi: 10.1038/s41467-022-29484-1)
- 372 [28] Mousanezhad, D., Haghpanah, B., Ghosh, R., Hamouda, A.M., Nayeb-Hashemi, H. and
373 Vaziri, A., 2016. Elastic properties of chiral, anti-chiral, and hierarchical honeycombs: A simple
374 energy-based approach. *Theoretical and Applied Mechanics Letters*, 6(2), pp.81-96. (doi:
375 10.1016/j.taml.2016.02.004)

376 [29] Bodaghi, M., Damanpack, A.R., Hu, G.F. and Liao, W.H., 2017. Large deformations of soft
377 metamaterials fabricated by 3D printing. *Materials & Design*, 131, pp.81-91. (doi:
378 10.1016/j.matdes.2017.06.002)

379 [30] Zhang, Y., Ren, X., Jiang, W., Han, D., Zhang, X.Y., Pan, Y. and Xie, Y.M., 2022. In-plane
380 compressive properties of assembled auxetic chiral honeycomb composed of slotted wave plate.
381 *Materials & Design*, 221, p.110956. (doi: 10.1016/j.matdes.2022.110956)

382 [31] Grima, J.N., Gatt, R., Alderson, A. and Evans, K.E., 2005. On the potential of connected stars
383 as auxetic systems. *Molecular Simulation*, 31(13), pp.925-935. (doi: 10.1080/08927020500401139)

384 [32] Xu, N. and Liu, H.T., 2020. A novel 3-D structure with tunable Poisson's ratio and adjustable
385 thermal expansion. *Composites Communications*, 22, p.100431. (doi: 10.1016/j.coco.2020.100431)

386 [33] Gong, X., Ren, C., Sun, J., Zhang, P., Du, L. and Xie, F., 2022. 3D Zero Poisson's Ratio
387 Honeycomb Structure for Morphing Wing Applications. *Biomimetics*, 7(4), p.198. (doi:
388 10.3390/biomimetics7040198)

389 [34] Rajabi, H., Eraghi, S.H., Khaheshi, A., Toofani, A., Hunt, C. and Wootton, R.J., 2022. An
390 insect-inspired asymmetric hinge in a double-layer membrane. *Proceedings of the National Academy*
391 *of Sciences*, 119(45), p.e2211861119. (doi: 10.1073/pnas.2211861119)

392 [35] Ma, Z., Lin, J., Xu, X., Ma, Z., Tang, L., Sun, C., Li, D., Liu, C., Zhong, Y. and Wang, L., 2019.
393 Design and 3D printing of adjustable modulus porous structures for customized diabetic foot
394 insoles. *International Journal of Lightweight Materials and Manufacture*, 2(1), pp.57-63. (doi:
395 10.1016/j.ijlmm.2018.10.003)

396 [36] Dong, L., Wang, D., Wang, J., Jiang, C., Wang, H., Zhang, B., Wu, M.S. and Gu, G., 2022.
397 Modeling and Design of Periodic Polygonal Lattices Constructed from Microstructures with
398 Varying Curvatures. *Physical Review Applied*, 17(4), p.044032. (doi:
399 10.1103/PhysRevApplied.17.044032)

400 [37] Jafarpour, M., Gorb, S. and Rajabi, H., 2023. Double-spiral: a bioinspired pre-programmable
401 compliant joint with multiple degrees of freedom. *Journal of the Royal Society Interface*, 20(198),
402 p.20220757. (doi: 10.1098/rsif.2022.0757)

403 [38] Tsuji, K. and Müller, S.C., 2019. *Spirals and Vortices: In Culture, Nature, and Science* (p.296). Cham,
404 Switzerland: Springer. (doi: 10.1007/978-3-030-05798-5)

405 [39] Smith M. 2009. *Abaqus/standard user's manual, version 6.9*. Providence, RI: Dassault Systèmes
406 Simulia Corp.

407 [40] Fillamentum, and addi(c)tive polymers. 2019. Flexfill TPU 98A Technical Data Sheet.

408 [41] Pinskiar, J., Shirinzadeh, B., Ghafarian, M., Das, T.K., Al-Jodah, A. and Nowell, R., 2020.

409 Topology optimization of stiffness constrained flexure-hinges for precision and range

410 maximization. *Mechanism and Machine Theory*, 150, p.103874. (doi:

411 10.1016/j.mechmachtheory.2020.103874)

412 [42] Eraghi, S.H., Toofani, A., Khaheshi, A., Khorsandi, M., Darvizeh, A., Gorb, S. and Rajabi, H.,

413 2021. Wing coupling in bees and wasps: From the underlying science to bioinspired engineering.

414 *Advanced Science*, 8(16), p.2004383. (doi: 10.1002/advs.202004383)

415 [43] Khaheshi, A., Gorb, S.N. and Rajabi, H., 2021. Spiky-joint: a bioinspired solution to combine

416 mobility and support. *Applied Physics A*, 127(3), pp.1-7. (doi: 10.1007/s00339-021-04310-5)

417 [44] Rawat, P., Zhu, D., Rahman, M.Z. and Barthelat, F., 2021. Structural and mechanical properties

418 of fish scales for the bio-inspired design of flexible body armors: A review. *Acta Biomaterialia*,

419 121, pp.41-67. (doi: 10.1016/j.actbio.2020.12.003)

420 [45] Khaheshi, A., Tramsen, H.T., Gorb, S.N. and Rajabi, H., 2021. Against the wind: A load-

421 bearing, yet durable, kite inspired by insect wings. *Materials & Design*, 198, p.109354. (doi:

422 10.1016/j.matdes.2020.109354)

423

424 **Tables**




425 **Table 1.** Mechanical properties of the thermoplastic polyurethane filament (Flexfill TPU 98A,
 426 Fillamentum addi©tive polymers, Czech Republic) [40].

Density (kg/m ³)	
1230	
Poisson's ratio	
0.3	
Stress (MPa)	Strain
0	0
12.1	0.1
22.1	0.5
28.4	1.0
37.8	3.0

427

428

Table 2. Double-spiral models developed for 3D printing, besides their corresponding values of design variables, and settings used for 3D printing.

3D modeling				
Developed double-spirals		Double-spiral 1	Double-spiral 2	Double-spiral 3
				
Design variables	Polar slope	0.10	0.20	0.05
	Initial thickness (mm)	3.0	2.5	1.0
	Angle of rotation (rad)	3π	1.5π	4π
	Extrusion height (mm)	20	20	20
3D printing settings				
Filament type		Thermoplastic polyurethane		Polylactic acid
Filament name		Flexfill TPU 98A		PLA
Produced by		Fillamentum addi(c)tive polymers, Czech Republic		Prusa Research, Praha, Czech Republic
Filament diameter (mm)		1.75		1.75
Nozzle diameter (mm)		0.4		0.4
Extrusion temperature (°C)		240		215
Bed temperature (°C)		50		60
Layer height (mm)		0.2		0.2
Fill pattern		Gyroid		Gyroid
Fill density (%)		20		20

435 **Figure captions**

436 **Fig 1.** Development of the 2D model of the double-spirals and four-module metastructure. a)
437 Plotting four spiral curves to generate two spiral surfaces for developing double-spiral 1. b) Double-
438 spiral 1 and 2 models. c) A modular metastructure consisted of double-spiral modules connected
439 to blocks. d) Employing double-spirals 1 and 2 to develop a four-module metastructure.

440 **Fig 2.** Simulation of the mechanical behavior of the four-module metastructure model. Results are
441 given for the following loading scenarios: in-plane a) tension, b) compression, c) rotation, and d)
442 sliding. Shaded areas show the fixed boundary conditions, and arrows show the direction of the
443 applied loads.

444 **Fig 3.** 3D printing and testing two double-spirals from the numerical simulations. Comparison of
445 the force–displacement curves and force values obtained from the numerical and experimental
446 tensile tests on the double-spirals 1 and 2.

447 **Fig 4.** 3D printing and testing a beam-like modular metastructure. Eight structures were developed
448 using double-spirals 1 and 2 arranged in eight different ways. The structures were fixed at one end
449 and a 250-N.mm moment was applied to their free end. Shaded area shows the fixed boundary
450 condition, and the arrow shows the direction of the applied moment. The deflections of the loaded
451 structures can be compared using the displacement values written next to the blocks and the
452 diagrams illustrating their deflections all together.

453 **Fig 5.** 3D printing and testing a cubic modular metastructure. a) three cubes were developed using
454 double-spirals 1, 2, and 3. b) The third cube was placed between two plates, and a 100-N force was
455 used to displace one plate towards the other one that was fixed. The force-displacement diagrams
456 show the anisotropic behavior of the cubic metastructure in x, y, and z directions.

457

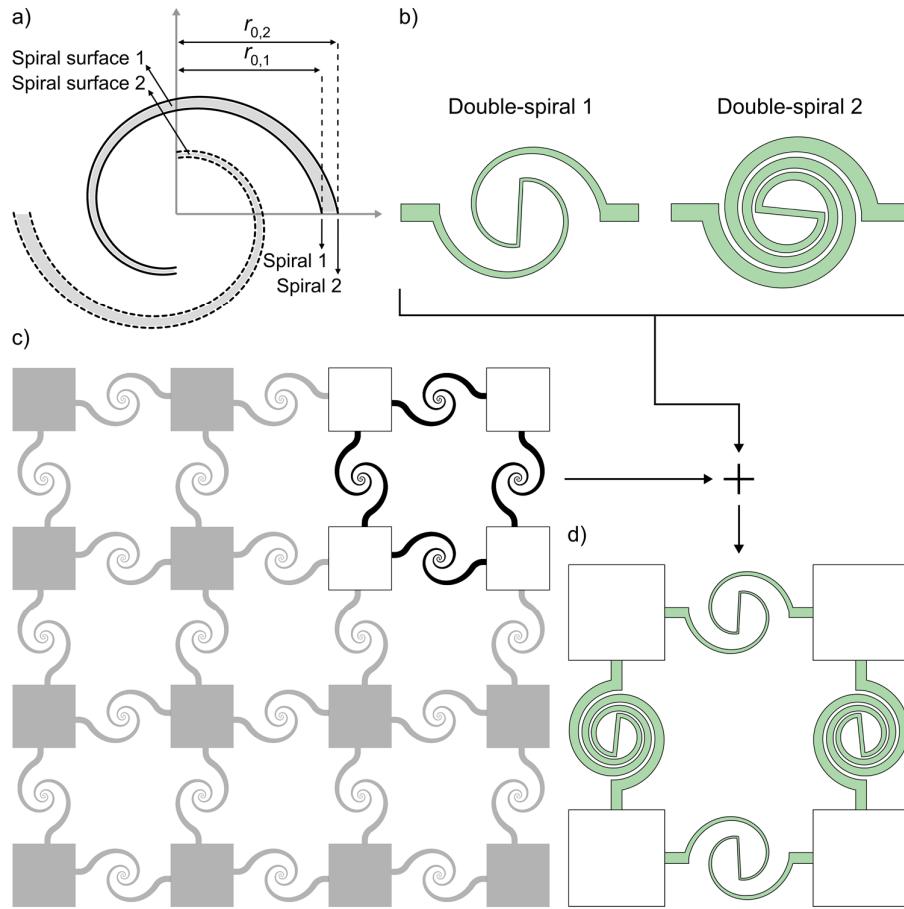


Fig 1. Development of the 2D model of the double-spirals and four-module metastructure. a) Plotting four spiral curves to generate two spiral surfaces for developing double-spiral 1. b) Double-spiral 1 and 2 models. c) A modular metastructure consisted of double-spiral modules connected to blocks. d) Employing double-spirals 1 and 2 to develop a four-module metastructure.

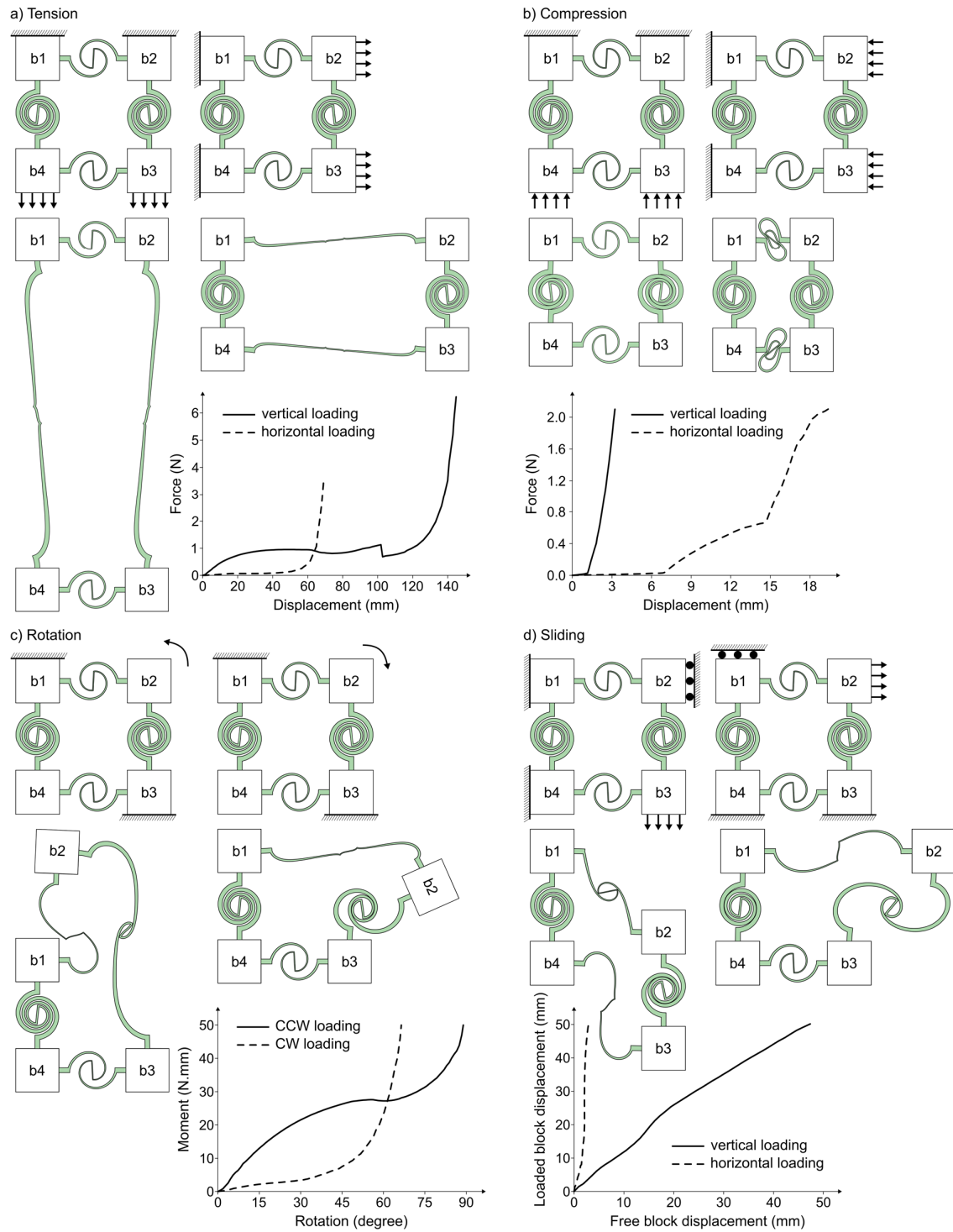


Fig 2. Simulation of the mechanical behavior of the four-module metastructure model. Results are given for the following loading scenarios: in-plane a) tension, b) compression, c) rotation, and d) sliding. Shaded areas show the fixed boundary conditions, and arrows show the direction of the applied loads.

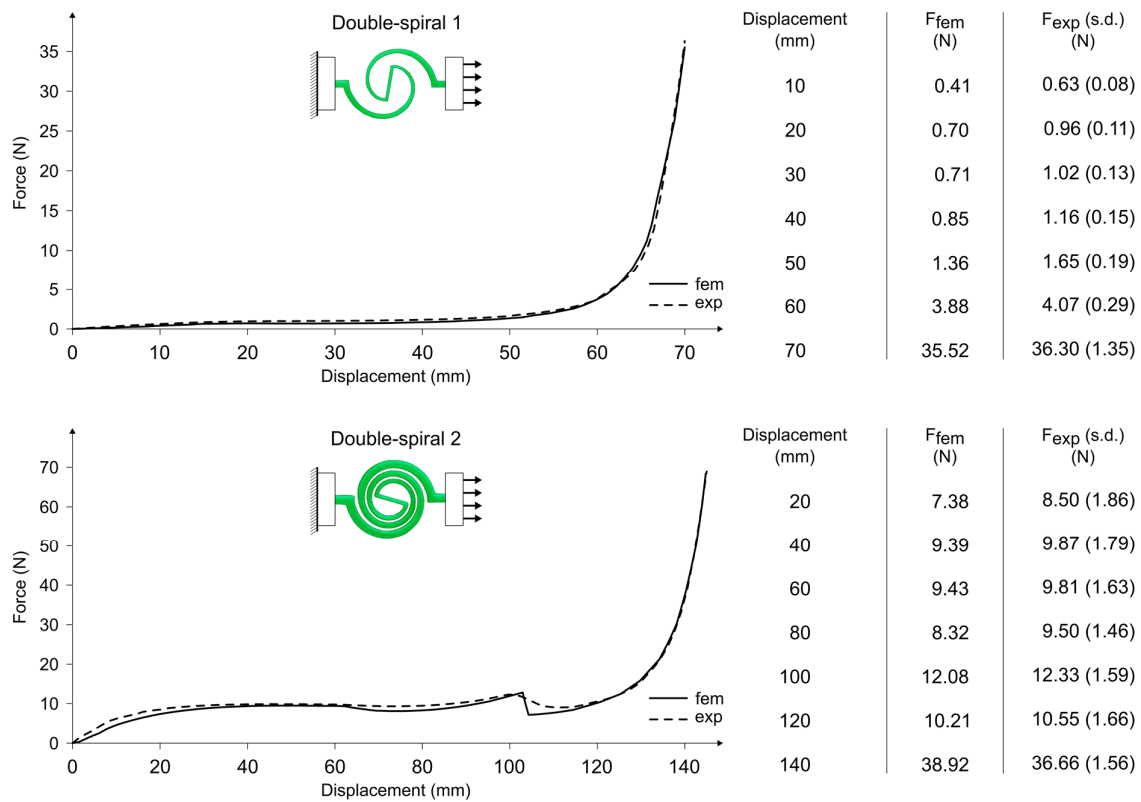


Fig 3. 3D printing and testing two double-spirals from the numerical simulations. Comparison of the force-displacement curves and force values obtained from the numerical and experimental tensile tests on the double-spirals 1 and 2.

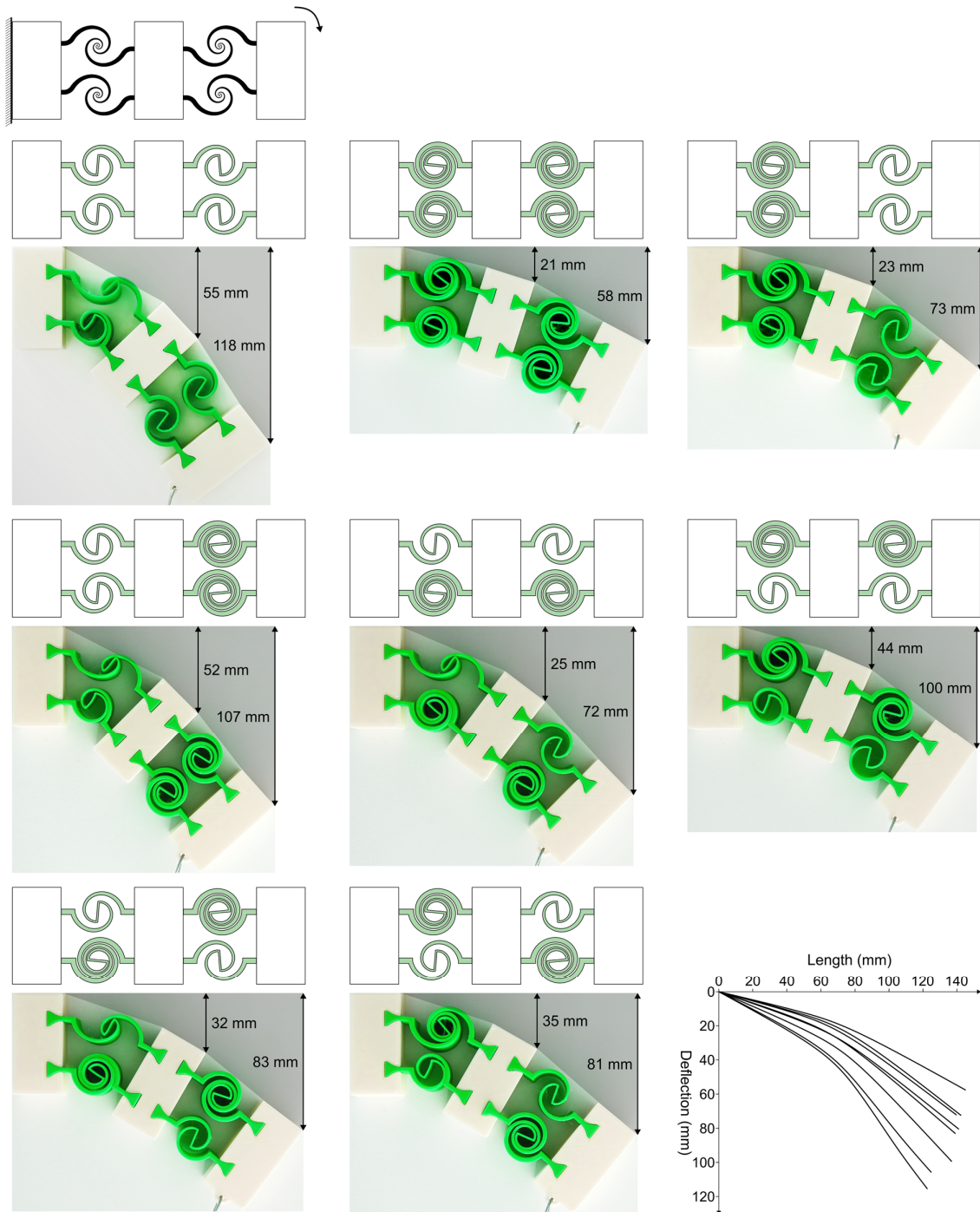


Fig 4. 3D printing and testing a beam-like modular metastructure. Eight structures were developed using double-spirals 1 and 2 arranged in eight different ways. The structures were fixed at one end and a 250-N.mm moment was applied to their free end. Shaded area shows the fixed boundary condition, and the arrow shows the direction of the applied moment. The deflections of the loaded structures can be compared using the displacement values written next to the blocks and the diagrams illustrating their deflections all together.

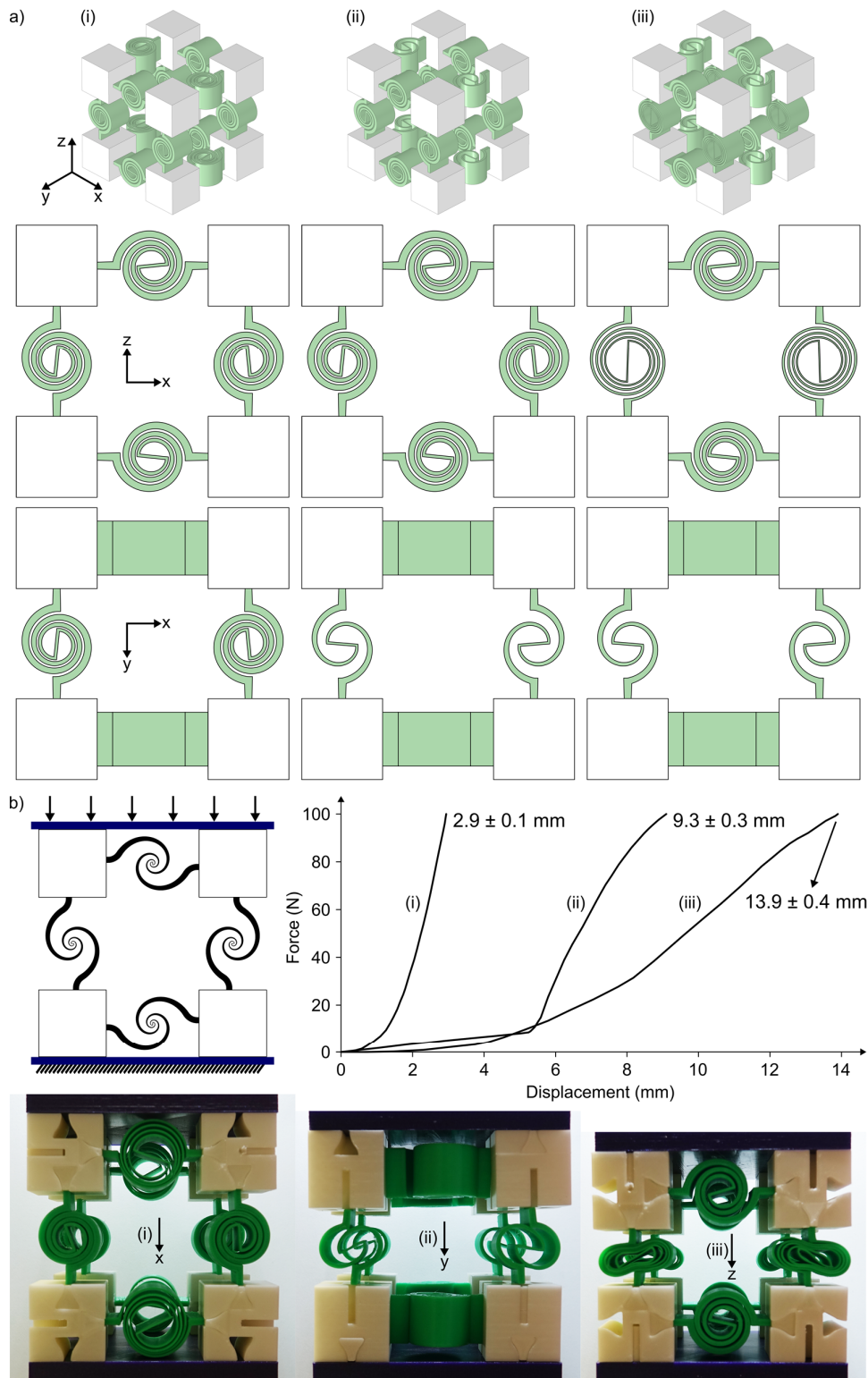


Fig 5. 3D printing and testing a cubic modular metastructure. a) three cubes were developed using double-spirals 1, 2, and 3. b) The third cube was placed between two plates, and a 100-N force was used to displace one plate towards the other one that was fixed. The force-displacement diagram shows the anisotropic behavior of the cubic metastructure in x, y, and z directions. The average values of the maximum displacement ($n=5$) and their standard deviations are written next to the corresponding curves.